Innovative Training Networks (ITN)
Call: H2020-MSCA-ITN-2017

MultidisciplinarY training network for ATrial fibRillation monItoring, treAtment and progression

Project Nº: 766082

Start date of the project: 01/11/2017

Duration: 48 months

Project Coordinator: Luca Mainardi

Deliverable D5.12

D5.12: Final Conference Report

Submission date: 31/10/2021

This project has received funding from the European Union's Horizon 2020 research and Innovation programme under the Marie Skłodowska-Curie grant agreement No 766082.

Document Properties

Document ID	D5.12
Document Title	Final Conference Report
Deliverable Nº	D29
Editors	Valentina Corino, Luca Mainardi
Contributors	All
Lead Beneficiary	POLIMI
Work Package Nº	5
Work Package Title	Training and transfer of knowledge
Nature	Report
Dissemination Level	Public
Number of pages	33
Due Date (in months)	48
Submission date	31/10/2021

Distribution List

Organization	Name of recipients
POLIMI	Luca Mainardi, Josè Felix Rodriguez Matas, Valentina Corino
UMIL	Roberto Sassi
LU	Leif Sörnmo
UNIZAR	Pablo Laguna
UPV	Javier Saiz
KIT	Olaf Doessel
MEDTRONIC BRC	Mirko De Melis
MIE	Johan De Bie
GRAD	Helena Fernandez
EMP	Francesco Onorati
KH	Claus Schmitt
HIC	Damian Sanchez-Quintana
SKANE	Pyotr Platonov
OMP	Federico Lombardi
ESR Representatives	Guadalupe Garcia Isla, Giorgio Luongo

Revision History

Rev. No.	Date of Issue	Author(s)	Brief Description of Change
0.9	25.10.2021	Valentina Corino	First draft
1.0	30.10.2021	Valentina Corino, Luca Mainardi, All	Final draft

Table of contents

1. Summary

This document describes the activities of the Final Conference of the MY-ATRIA consortium. The conference was hosted by University of Karlsruhe at the KIT Campus in Karlsruhe, Germany. The event provided opportunities for the ESRs and practice of conference-like communication, as each of them presented his/her work orally.

2. Summer school objectives and agenda

The objectives of the Final Conference was for ESRs to present their project and to receive feedback from other ESRs and supervisors. In particular, the ESRs were asked to present their work like an extended “pitch”.

The meeting was on September 26, 2021, see agenda below.

Sunday, 26 September 2021		
TIME	**ACTIVITY**	**RESPONSIBLE/SPEAKER**
8:45	**Welcome**	Luca Mainardi (POLIMI) & Olaf Dössel (KIT)
9:00	**ESR1: Bottom-up study on the implications of interatrial block in the mechanisms of atrial fibrillation**	Jordan Eliot (POLIMI)
9:20	**ESR2: Detailed 3-D computer models of human atria and torso for studying atrial fibrillation initiation and progression**	Rebecca Belletti (UPV)
9:40	**ESR3: Body Surface Potential Maps and ECG-signals of Atrial Fibrillation**	Giorgio Luongo (KIT)
10:00	**ESR4: Atrial complex networks in endocavitary recordings during Atrial Fibrillation**	Muhamed Vila (UMIL)
10:20	**Coffee break**	
10:40	**ESR5: Paroxysmal atrial fibrillation (PAF): continuous tracking of arrhythmia progression**	Ricardo Salinas Martínez (MIE)
11:00	**ESR6: Atrial fibrillation screening using everyday sensors and data fusion (remote)**	Hesam Halvaei (LUND)
11:20	**ESR7: Risk stratification and prediction of intervention outcome in AF using novel ECG-based markers of atrial remodeling (remote)**	Mostafa Abdollahpur (LUND)
11:40	**ESR8: Assessment of the Atrial Fibrillation triggers and their role in its progression**	Francisco Javier Saiz Vivo (MEDTRONIC BRC)
12:00	**Lunch break**	
13:00	**ESR9: Evaluation of the interplay mechanism between AF and AT detected by a single lead ECG**	Guadalupe García Isla (POLIMI)
13:20	**ESR10: Integrated and personalized computational model of atria with AF for an efficient ablation therapy**	Luca Azzolin (KIT)
13:40	**ESR11: Assessment of Atrial Fibrillation therapies targeting ion channels and neural components**	Chiara Celotto (UNIZAR)
14:00	**ESR12: Characterization of Atrial Fibrillation (AF) dynamics for ablation guidance and prediction of its efficacy**	Jennifer Riccio (UNIZAR)
14:20	**Tea and coffee**	

Sunday, 26 September 2021		
TIME	**ACTIVITY**	**RESPONSIBLE/SPEAKER**
15:00	**Panel of the Project Leaders: Moving on from My-Atria to real benefit for the patient (3 min statements each + discussion)**	Mainardi, Dössel, Sassi, Loewe, Sandberg, Corino, Saiz, Rodriguez Matas
16:00	**My experiences when moving into medical industry after PhD**	Tobias Oesterlein (BOSTON SCIENTIFIC)
17:00	**Concluding remarks**	Luca Mainardi (POLIMI)
17:15	**Non-official Supervisory Board Meeting/** **… a walk through the park**	(MY-ATRIA Supervisory Board members only/ESRs+)
18:00	**Party on the IBT rooftop**	

3. ESR presentations

The ESR presentations were performed as an extended pitch for 10-min presentation followed by 10-min discussions, as shown in the Table at page 6. The ESRs and the supervisors participated in the discussions. The questions and related discussion were focused on the exploitability of their results.

The ESRs also summarized the work they presented in an abstract (see Annex 1).

4. Panel discussions

A panel discussion was organized after the ESR presentations (see Table page 7) to discuss what to do after the end of MY-ATRIA project from a research point of view as well as for dissemination, communication and exploitation of the obtained results. In this regard, it was decided to prepare a manuscript with the main results from MY-ATRIA to be published as part of an special issue of the Journal Medical and Biological Engineering and Computing.

5. Scientific lectures (day 2-3)

Tobias Oesterlein, who made his PhD in professor Doessel's lab is now working at Boston Scientific, gave a talk about his experiences while changing from academics to industry. The presentation was followed by a 20 minute discussion.

6. Summer school evaluation

An online survey, following the guidelines described in the Deliverable D5.4 "Evaluation Questionnaries M12" was created with Google Forms and completed by each ESR. The results of the survey were reported in the Deliverable D5.6 "Evaluation Questionnaries M24", due in month 24th.

7. Conclusions

The objective of the Final Event was to have the ESRs presenting their project and the main results.

Annex 1 – Abstract section

Cellular variability within the in-silico atria and its impacts on conduction velocity in healthy and AF remodeled tissue.

Jordan Elliott

Introduction

Atrial models are increasingly relied upon to understand the mechanisms behind atrial arrhythmias such as atrial fibrillation. In order to represent the behaviour of the atria, it is important to create representative models of the human atria. Due to difficulties incorporating cellular variability, models typically assume cellular coupling masks the impact of electrophysiological variability on the cellular level. Electrophysiological models typically only vary at a regional level. Recent studies have shown that cellular variability may have a larger impact on electrophysiological behaviour than previously expected.

Material and Methods

A population of unique cellular models was created using the Courtemanche cellular model. Published experimental data was used to divide the population into 8 regional populations based on 5 biomarkers (RMP, APA, APD20, APD50, APD90). Regionally homogenous and heterogeneous tissue samples were separately calibrated to target experimental CV values. The variability in CV across 10 heterogeneous models were compared for each atrial region. Activation maps and APD maps were calculated for whole atria simulations of the regionally homogenous and heterogeneous models.

Results

Isolated heterogeneous tissue results using the same tissue conductance showed the standard deviation in CV ranged from 0.19cm/s to 2.4cm/s depending on atrial region. Similar variability in CV was observed between healthy and AF remodelled tissue samples. Figure 1 shows the regional variability in CV across the 10 heterogeneous models. In the healthy atria, whole atrial simulations showed heterogeneous models resulted in a similar average total activation times (TAT) compared with the regionally homogenous model (117ms), varying between 117ms and 118ms. Depolarization across the regionally homogenous model and the variable models remained consistent for both the healthy and AF remodelled atria. Repolarization in the variable atrial models was faster than in the homogenous model.

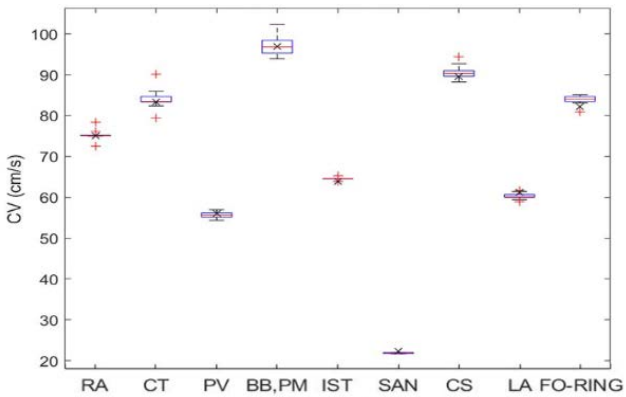

Figure 1 Boxplot showing variability in CV across AF remodeled atrial regions due to cellular variability.

Discussion and Conclusions

Cellular variability across isolated tissue results in CV variation of up to 4cm/s. Unsurprisingly, electrophysiological variability has a negligible impact on depolarization across the atria. Most of the observed variability in activation times is caused by anatomical variability. Electrophysiological variability results in an earlier and faster repolarization phase for both the healthy and AF remodelled atria. This could have a significant impact on the susceptibility to the maintenance of AF episodes. Accounting for cellular variability could result in models better representing healthy atrial behaviour and that of different arrhythmias.

Arrhythmogenicity of genetic mutations on a 3D human atrial model

Rebecca Belletti

Introduction

Atrial fibrillation (AF) is the most frequent supra-ventricular arrhythmia and it has been related to the presence of genetic defects in genes encoding potassium channel protein structures in otherwise healthy patients. The arrhythmogenicity of three genetic mutations - KNCH2 T436M, KCNH2 T895M and KCNE3-V17M - has been previously studied at the cellular and tissue levels. The aim of this study is to investigate the pro-arrhythmogenic effects of such mutations by modeling and simulating its electrical activities on a 3D atrial geometry.

Material and Methods

The 3D hexahedral mesh, representing the human atrial model, is characterized by 21 regions and 56 subregions to account for heterogeneous histological properties and fiber orientation, and by a spatial resolution of 300 µm. The cellular electrical activity was modelled using a modified version of the Courtemanche-Ramirez-Nattel model, which includes both the formulation of the acetylcholine-activated potassium current and the parameters reproducing the genetic mutations' effects. Nine ionic models were implemented by tuning several ionic conductances to account for regional electrical properties. Longitudinal conductivities and anisotropy ratios were also tuned in each region to reproduce tissue heterogeneities and activation sequences. The electrical models were stabilized by applying 10 continuous beats to the sinoatrial node (SAN) with a 1000 ms basic cycle length (BCL). To get re-entrant activity, a train of 5 stimuli was applied to the coronary sinus (CS) region with a BCL of 160 ms for the mutation KCNH2 T436M, of 170 ms for KCNH2 T895M, and of 90 ms for the mutation KCNE3-V17M. During the CS pacing, the SAN was simultaneously stimulated by a 5-pulse train with BCL of 1000 ms. Temporal vulnerability to re-entrant activity for each mutation was computed as the width of the window when a train of stimuli in the CS would elicit a re-entry.

Results

The presence of the mutations increased the vulnerability of the atria to reentry and different types of arrhythmic behavior were observed. The KCNH2 T436M mutation presented a vulnerable window (VW) of 10 ms, and mostly macro-reentries and rotors, generated in the right atrium (RA) and perpetuated for a minimum of 3.8 s and for a maximum of 5 s. In the presence of the mutation KCNH2 T895M, the VW has a 7 ms-width, and was characterized by the appearance of mostly macro-reentries perpetuating until the end of the simulations (5s). Finally, the VW for the KCNE3-V17M mutation was 24 ms-wide. In this case, all the rotors appeared in the CS area, moved around the RA walls and were sustained for the remaining simulation time. Collisions of

multiple waves led to the formations of several instable rotors in both right and left atrium, wave breaks and to an overall more complex arrhythmogenic pattern.

Discussion and Conclusions

This preliminary study supports that the presence of the genetic mutations in 3D human atrial model resulted in a more arrhythmogenic substrate, leading to mutation-dependent forms of arrhythmias.

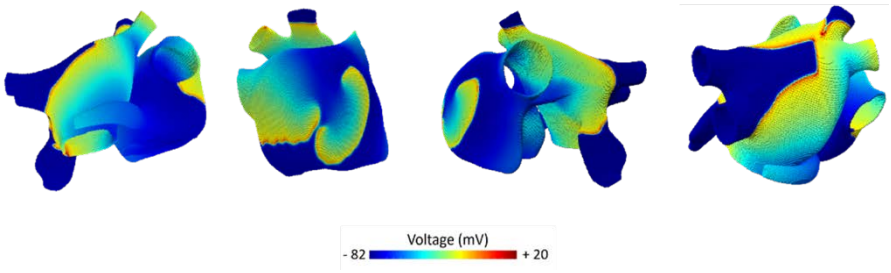

Figure 2: Simulation of complex spiral waves in 3D human atria in presence of the KCNE3-V17M mutation.

References

1. *Ferrer, A., Sebastián, R., Sánchez-Quintana, D., Rodríguez, J. F., Godoy, E. J., Martínez, L., et al. (2015). Detailed anatomical and electrophysiological models of human atria and torso for the simulation of atrial activation. PLoS One. doi: 10.1371/journal.pone.0141573*
2. *Courtemanche, M., Ramirez, R. J., and Nattel, S. (1998). Ionic mechanisms underlying human atrial action potential properties: insights from a mathematical model. Am. J. Physiol. Heart Circ. Physiol. 275, 301–321. doi: 10.1152/ajpheart.1998.275.1.H301*
3. *Grandi, E., Pandit, S. V., Voigt, N., Workman, A. J., Dobrev, D., Jalife, J., et al. (2011). Human atrial action potential and Ca 2+ model: sinus rhythm and chronic atrial fibrillation. Circ. Res. 109, 1055–1066. doi: 10.1161/CIRCRESAHA.111.253955*
4. *Rocher, S., Martinez, L., Lopez, A., Ferrer, A., Sanchez-Quintana, D., & Saiz, J. (2019). A Three-Dimensional Model of the Human Atria With Heterogeneous Thickness and Fibre Transmurality - A Realistic Platform for the Study of Atrial Fibrillation. 2019 Computing in Cardiology Conference (CinC), 45, 2019 – 2022. https://doi.org/10.22489/cinc.2019.380*
5. *Belletti, R., Romero, L., Martinez-Mateu, L., Cherry, E. M., Fenton, F. H., & Saiz, J. (2021). Arrhythmogenic Effects of Genetic Mutations Affecting Potassium Channels in Human Atrial Fibrillation: A Simulation Study. Frontiers in Physiology, 12(May), 1–16. https://doi.org/10.3389/fphys.2021.681943*

Hybrid Machine Learning to Localize Atrial Flutter Substrates Using the Surface 12-lead ECG

Giorgio Luongo

Introduction

Atrial flutter (AFlut) is a common reentrant atrial tachycardia driven by self-sustainable mechanisms that cause excitations to propagate along pathways different from sinus rhythm. Intracardiac electrophysiological mapping and catheter ablation are often performed without detailed prior knowledge of the mechanism perpetuating AFlut, likely prolonging the procedure time of these invasive interventions. We sought to discriminate the AFlut location (cavotricuspid isthmus-dependent, peri-mitral, and other left atrium AFlut classes) with a machine learning-based algorithm using only the non-invasive signals from the 12-lead electrocardiogram (ECG).

Material and Methods

A hybrid 12-lead ECG dataset of 1,703 signals was used (1,424 in-silico ECGs, and 279 clinical ECGs from 93 patients – 3 different ECG segments over time were extracted from each patient). For each ECG, 77 features were extracted. A decision tree classifier with a hold-out classification approach was trained, validated, and tested on the dataset randomly split after selecting the most informative features. The clinical test set comprised 15 patients (45 clinical ECGs).

Results

The classifier yielded 82.2% accuracy on the clinical test set with a sensitivity of 90.9%, 66.7%, and 50.0% and a positive predictive value of 85.7%, 66.7%, and 75.0% for each class, respectively. Considering majority vote of the three segments taken from each patient, the cavotricuspid isthmus-dependent class was always classified correctly.

Discussion and Conclusions

Our results show that a machine learning classifier relying only on non-invasive signals can potentially identify the location of AFlut mechanisms. This method could aid in planning and tailoring patient specific AFlut treatments.

References

[1] G. Luongo *et al.*, "Hybrid Machine Learning to Localize Atrial Flutter Substrates Using the Surface 12-lead ECG," *Under Rev.*, 2021.

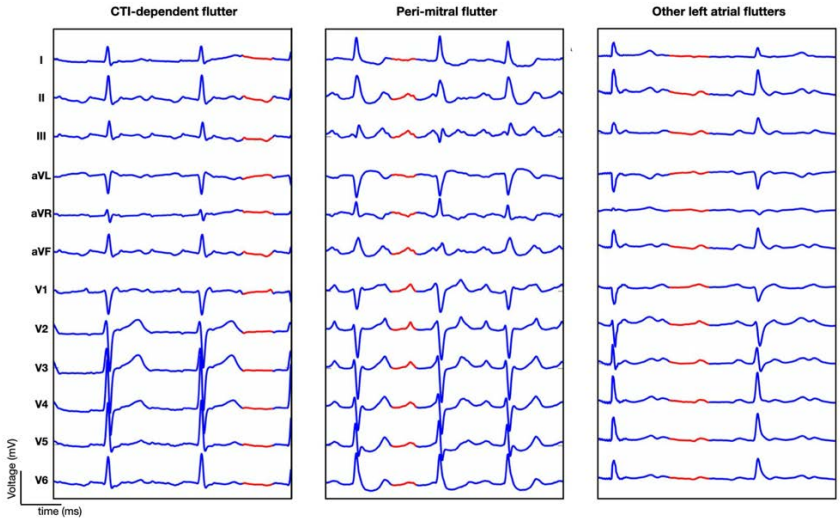

Figure 3: Example of clinical CTI-dependent, peri-mitral, and other LA AFlut 12-lead ECGs, respectively. The red segments represent one of the three AFlut single cycles extracted and used in this work for this specific patient [1].

Directed Network Mapping Hints the Ablation Strategy for Atrial Flutter: A Proof of Concept

Muhamed Vila

Introduction

Atrial flutter (AFL) is typically characterized by electrical activity propagating around specific anatomical regions and it is usually treated with catheter ablation. In this study, we modeled the electrical propagation pattern of AFL using directed network mapping (DNM). DNM is a recent method that makes use of network theory (NT) to characterize the electrical propagation [1,2], such as the identification of cycles and focal points. The network is composed by nodes and edges resembling electrodes located across the atrial surface and the direction of the electrical propagation from one electrode to another. The aim of the study was to verify whether DNM can recommend an ablation strategy to stop the mechanism generating AFL.

Material and Methods

To test the algorithm, we set up a computational scenario based on a simulated AFL around the mitral valve in counterclockwise direction, as implemented in a previous work [3]. Electrograms and 3D anatomy were used in the DNM algorithm to build the network *N*. Then, electrical cycles were detected using a standard network search algorithm. In order to recommend ablation lines in an automatic fashion we proceeded as follows. First, a second network *A*, based on the Voronoi tessellation, was built on top of *N* in such a way that the edges connecting the nodes of *A* would cross the edges of *N* (thus resembling an ablation line capable of interrupting the electrical propagation between two connected electrodes). A list of all possible ablation lines from the network *A* was built using an implementation of the shortest path algorithm. Then, among these, we determined those capable, by themselves, of stopping the electrical cycles (and possibly the AFL).

Results

We identified all the ablation lines capable of interrupting, at the same time, every cycle detected in *N*. An example is in Figure 1.

Discussion and Conclusions

We proposed a proof-of-concept algorithm, based on DNM, to automatically recommend ablation lines for the treatment of AFL.

References

[1] Vandersickel, N. et al., “Directed networks as anovel way to describe and analyze cardiac exci-tation: Directed graph mapping,”Front Physiol,vol. 10, p. 1138, 2019.

[2] Vila, M. et al., “Directed network mapping ap-proach to rotor localization in atrial fibrillationsimulation,” inConf Proc IEEE Eng Med BiolSoc, 2021.

[3] Luongo, G. et al., “Non-invasive characteriza-tion of atrial flutter mechanisms using recurrencequantification analysis on the ECG: A computa-tional study,”IEEE Trans Biomed Eng, vol. 68,pp. 914–925, 1 2021.

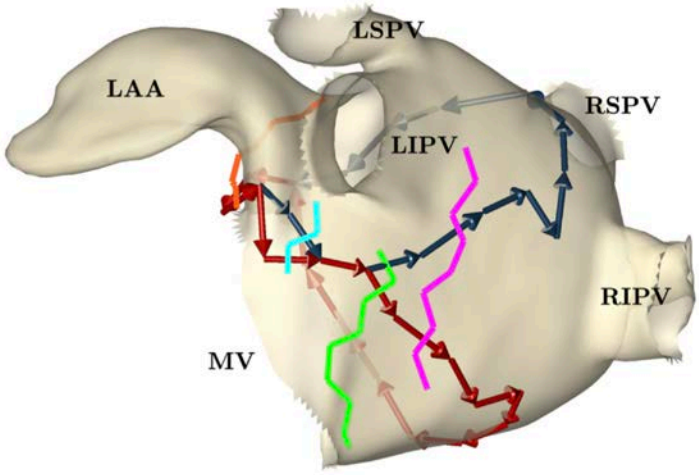

Figure 1: 3D model of the left atrium along withthe detected cycles (red and blue arrows) and ab-lation lines (magenta, green, cyan, and orange).

Detection of Brief Episodes of Atrial Fibrillation Based on Electrocardiomatrix and Convolutional Neural Network

Ricardo Salinas-Martínez

Introduction

Brief episodes of atrial fibrillation (AF) may evolve into longer AF episodes increasing the chances of thrombus formation, stroke, and death.[1] Classical methods for AF detection investigate rhythm irregularity or P-wave absence in the ECG, while deep learning approaches profit from the availability of annotated ECG databases to learn discriminatory features linked to different diagnosis. However, some deep learning approaches do not provide analysis of the features used for classification. This paper introduces a convolutional neural network (CNN) approach for automatic detection of brief AF episodes based on electrocardiomatrix-images[2] (ECM-images) aiming to link deep learning to features with clinical meaning.

Material and Methods

The CNN is trained using two databases: the Long-Term Atrial Fibrillation and the MIT-BIH Normal Sinus Rhythm, and tested on three databases: the MIT-BIH Atrial Fibrillation, the MIT-BIH Arrhythmia, and the Monzino-AF. Detection of AF is done using a sliding window of 10 beats plus 3 s. Performance is quantified using both standard classification metrics and the EC57 standard for arrhythmia detection. Layer-wise relevance propagation[3] analysis was applied to link the decisions made by the CNN to clinical characteristics in the ECG.

Results

For all three testing databases, episode sensitivity was greater than 80.22, 89.66, and 97.45% for AF episodes shorter than 15, 30 s, and for all episodes, respectively.

Discussion and Conclusions

Rhythm and morphological characteristics of the electrocardiogram can be learned by a CNN from ECM-images for the detection of brief episodes of AF.

References

1. Hindricks, G. *et al.* 2020 ESC Guidelines for the diagnosis and management of atrial fibrillation developed in collaboration with the European Association for Cardio-Thoracic Surgery (EACTS). *Eur. Heart J.* **42**, 373–498 (2021).
2. Li, D. *et al.* Electrocardiomatrix: A new method for beat-by-beat visualization and inspection of cardiac signals. *J. Integr. Cardiol.* **1**, 124–128 (2015).
3. Bach, S. *et al.* On pixel-wise explanations for non-linear classifier decisions by layer-wise relevance propagation. *PLoS One* **10**, (2015).

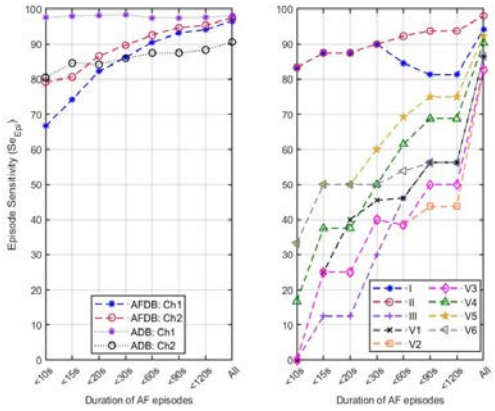

Figure 1: Episode sensitivity achieved on the episodes shorter than a particular duration present in: (left) channel 1 (Ch1) and channel 2 (Ch2) of the AFDB and Arrhythmia DB (ADB), respectively, and (right) leads I, II, III, V1, V2, V3, V4, V5, and V6 of the Monzino-AF DB.

Signal Quality Assessment of a Novel ECG Electrode for Motion Artifact Reduction

Hesam Halvaei

Introduction

The presence of noise is problematic in the analysis and interpretation of the ECG, especially in ambulatory monitoring. Restricting the analysis to high quality signal segments only comes with the risk of excluding significant arrhythmia episodes. Therefore, the development of novel electrode technology, robust to noise, continues to be warranted.

Material and Methods

The signal quality of a novel wet ECG electrode (Piotrode) is assessed and compared to a commercially available, commonly used electrode (Ambu). The assessment involves indices of QRS detection and atrial fibrillation detection performance, as well as signal quality indices (ensemble standard deviation and time–frequency repeatability), computed from ECGs recorded simultaneously from 20 healthy subjects performing everyday activities.

Results

The QRS detection performance using the Piotrode was considerably better than when using the Ambu, especially for running but also for lighter activities. For the Piotrode, no false AF detections are observed during running, i.e., the most physically demanding activity. On the other hand, for the Ambu, AF is falsely detected in 7 out of 20 subjects, with an FPR ranging from 36% to 100%. The two signal quality indices demonstrated similar trends: the gap in quality became increasingly larger as the subjects became increasingly more active. One example of the difference in signal quality between the Piotrode and the Ambu during running is illustrated (Fig. 1)

Discussion and Conclusions

The novel wet ECG electrode produces signals with less motion artifacts, thereby offering the potential to reduce the review burden, and accordingly the cost, associated with ambulatory monitoring.

References

1. *Petrenas, A.; Marozas, V.; Sörnmo, L. Low-complexity detection of atrial fibrillation in continuous long-term monitoring. Comput.*
2. *Biol. Med. 2015, 65, 184–191.*
3. *Martínez, J.P.; Almeida, R.; Olmos, S.; Rocha, A.P.; Laguna, P. A wavelet-based ECG delineator: Evaluation on standard databases.*
4. *IEEE Trans. Biomed. Eng. 2004, 51, 570–581.*
5. *Sörnmo, L.; Laguna, P. Bioelectrical Signal Processing in Cardiac and Neurological Applications; Elsevier (Academic Press): Amsterdam, The Netherlands, 2005.*
6. *Yaghmaie, N.; Maddah-Ali, M.A.; Jelinek, H.F.; Mazrbanrad, F. Dynamic signal quality index for electrocardiograms. Physiol.Meas. 2018, 39, 105008.*

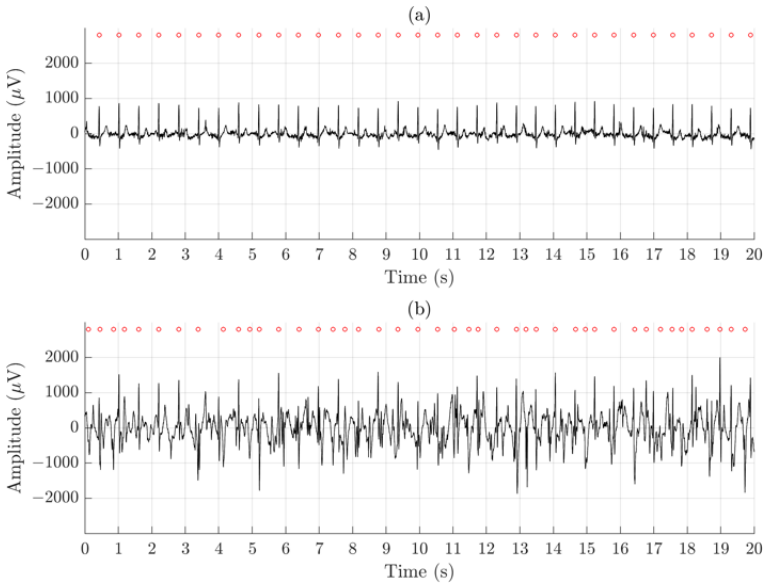

Figure 4 An example of signal recorded simultaneously during running using (a) the Piotrode and (b) the Ambu electrodes

A Subspace Projection Approach to Quantify Respiratory Variations in the f-wave Frequency Trend - Preliminary Results from SCAPIS

Mostafa Abdollahpur

Introduction

The autonomic nervous system (ANS) is an important factor in initiation and maintenance of atrial fibrillation (AF). However, methods for ECG based analysis of autonomic reactivity during AF are lacking. There are two primary aims of this study: 1. To propose a novel subspace projection approach to quantify respiratory variation in the f-wave frequency trend. 2. To investigate the impact of deep breathing on the f-wave frequency and the magnitude of respiratory variation in the f-wave frequency, respectively.

Materials and Methods

The study population consists of 28 participants from the Swedish cardiopulmonary bioimage study (SCAPIS) [1] that were diagnosed with AF. The ECG from these patients was recorded for 5 minutes at baseline and 1 minute during deep breathing; the patients were in AF during the recordings. The f-wave signal was extracted from ECGs by means of spatiotemporal qrst-cancellation [2], and a harmonic model was fitted to the f-wave to estimate a high resolution f-wave frequency trend ($\hat{f}(n)$) and a signal quality index (S) quantifying the model fit [3]. A respiration signal was extracted from each ECG lead separately using the slop rage method [4]. In order to identify one respiration signal and merge all information from the respiration signals, principal component analysis (PCA) was used. The PCA components accounting for more than 10% of the total variance and had a significant periodic component determined using Fisher's g-statistic [5] was selected as the respiration signal. Orthogonal subspace projection was applied to project the f-wave frequency trend onto the respiration subspace [6], the energy of the projected signal, $\mathrm{P_x}$, is used to quantify the magnitude of respiratory variation in the f-wave frequency.

Results

The signal quality was sufficient for estimation of the f-wave frequency (S>0.3) in 98% of the data. A respiration signal could be extracted from 92% of the analysed 1-minute segments obtained at baseline and 71% of the of the analysed 1-minute segments obtained during deep breathing. The changes of $\mathrm{P_x}$ from baseline to deep breathing is plotted versus the changes in mean f-wave frequency ($\bar{f}$) is displayed in Fig1. A large individual variation is observed in response to deep breathing, with changes in $\bar{f}$ ranging between -6% and 6%, and changes in $\mathrm{P_x}$ ranging between -60 % and 85 %.

Discussion and Conclusions

This study set out to introduce a subspace projection approach to quantify respiratory variation in the f-wave frequency. Preliminary results from analysis of SCAPIS data suggest that the approach is feasible.

References

1. Bergström, Göran, et al. "The Swedish cardiopulmonary BioImage study: objectives and design." *Journal of internal medicine* 278.6 (2015): 645-659.
2. Stridh, M., and L. Sörnmo. “Spatiotemporal QRST Cancellation Techniques for Analysis of Atrial Fibrillation.” IEEE transactions on bio-medical engineering 48.1 (2001): 105–111.
3. Henriksson, Mikael et al. “Model-Based Assessment of f-Wave Signal Quality in Patients with Atrial Fibrillation.” IEEE transactions on bio-medical engineering 65.11 (2018): 2600–2611.
4. Kontaxis, Spyridon, et al. "ECG-derived respiratory rate in atrial fibrillation." IEEE Transactions on Biomedical Engineering 67.3 (2019): 905-914.
5. Wichert, Sofia, Konstantinos Fokianos, and Korbinian Strimmer. "Identifying periodically expressed transcripts in microarray time series data." Bioinformatics 20.1 (2004): 5-20
6. Strang, G. "Linear Algebra and Its Applications (Belmont, CA: Thomson, Brooks/Cole)." (2006).

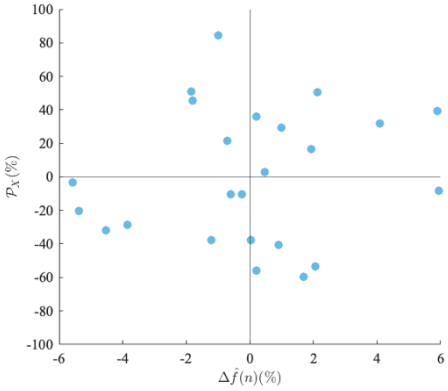

Fig5.The changes in P_x plotted versus the changes in $\Delta\bar{f}$ between baseline and deep breathing.

Effect of Extra Lesions on AF burden of Continuously Monitored Patients Undergoing Single-Procedure Catheter Ablation

Javier Saiz-Vivo

Introduction

Catheter Ablation (CA), specifically pulmonary vein isolation (PVI) is a well stablished procedure for patients suffering from Atrial Fibrillation (AF).

The effect of extra lesions on procedural outcome is unclear with studies suggesting there is reduction of AF recurrence. However, these studies relied heavily on 24-hour Holter recordings which have shown to have rather poor subclinical AF detection rates (5.5%) due to its intermittent nature. Furthermore, AF recurrence is considered as an ablation failure and AF bur-den reduction on the patients is not taken into consideration. Implantable cardiac monitors (ICMs) offer the advantage of continuous monitoring of the patient and offer high AF detection rates.

This study aims at evaluating the effect of extra lesions on the success rate of the procedure as well as on the AF burden change achieved on the patients.

Material and Methods

This retrospective study included 33 patients (67% male; 57 ± 12 years; 26% Non-Paroxysmal AF) which were implanted with the Reveal LINQ, an ICM with AF detection rates of up to 96% that continuously classifies the heart rhythm of the patient analyzing its cardiac cycle and stores the daily AF burden in minutes/day. The ICM was implanted 134 ± 97 days before the ablation procedures, which were classified as PVI or PVI plus extra lesions, and the patients were followed up for 223 ± 111 days.

The patients were also divided into two classes: those with AF recurrence, defined as those with a detected episode outside the 3-months blanking period, and those without.

Results

Of the 33 patients analyzed, 21 had PVI only and 12 had PVI plus extra lesions. From those with PVI only, 15 (71%) had AF recurrence with a median burden reduction of 83% out of which 8 (53%) had a burden reduction > 80%. From the patients which had PVI plus extra lesions, 10 (83%) had recurrence with a median burden reduction of 84% out of which 6 (60%) had a burden reduction > 80%. 6 patients had a median burden increase of 222%, out of which 3 underwent PVI plus extra lesions (median burden increase of 360%) and 3 had PVI only (median bur-den increase 83%).

Figure 1 shows the AF burden detected in minutes/day for the patients with AF recurrence divided into pre ablation (PRE), blanking period (BP) and post ablation (POST). The markings

show those patients that underwent PVI plus extra lesions (EL).

Discussion and Conclusions

Although a higher proportion of patients with PVI plus extra lesions had AF recurrence, a significant proportion of those with recurrence also had AF burden reduction > 80%. Moreover, for a small subgroup of patients in which the AF burden increased after CA, those with PVI plus extra lesions showed a higher increase in AF burden. This indicates that extra lesions could be indeed beneficial to some patients, especially in reducing the AF burden and, in doing so, increasing the quality of life of the patient.

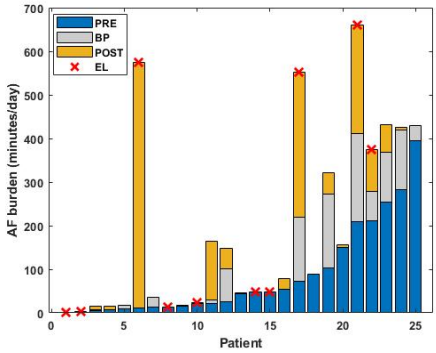

Figure 1: AF burden detected in patients with AF recurrence.

A Poincaré Image-Based Detector of ECG Segments Containing Atrial and Ventricular Beats

Guadalupe García-Isla

Introduction

An electrocardiogram (ECG) classifier for the detection of ECG segments containing atrial or ventricular (A/V) beats could ease in the detection of premature atrial complexes (PACs) and by so, the study of their relationship with atrial fibrillation (AF) and stroke [1]–[3]. In this work such a classifier is presented based on convolutional neural networks (CNN) and the RR and dRR interval representation on Poincaré Images.

Material and Methods

Two PhysioNet open-source databases containing beat annotations were used. ECG signals were divided into 30-beat segments with a 50% overlap. Each segment was then transformed into a Poinaré Image as in Figure 1. A total of 381151 and 62142 Poincaré Images were computed for normal (N) and A/V segments. RR, dRR and both types of Poincaré Images combined were evaluated as inputs to the CNN. The CNN was trained following a patient-wise train-test division (i.e., no patient was included both in the train and test set) in a 10-fold cross-validation.

Results

The patient-wise median and interquartile range accuracy, sensitivity and positive predictive values were 97.90 (94.49 - 99.28), 96.03 (89.67 - 98.76) and 91.91 (70.87 - 99.24), respectively for RR input. No statistical significant differences in performance were found among the three types of Poincaré Images input.

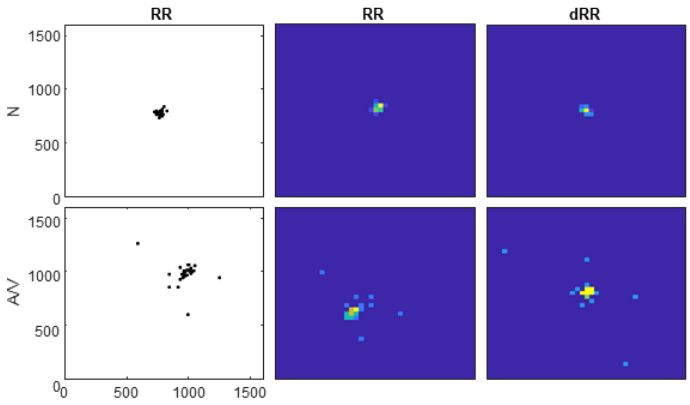

Figure 6. Poincaré Image RR and dRR representations of 30-beat ECG segments: 1st row containing only normal beats, 2nd column containing one or more atrial or ventricular beats (A/V).

Discussion and Conclusions

In this paper an ECG segment classifier is introduced for the detection of segments containing A/V beats. The results obtained suggest this methodology could be used to reduce the ECG beat annotation workload to study PACs and other A/V implications. In addition, it could be used in combination with automatic beat classifiers to find misclassifications and obtain more reliable annotations.

References

[1] B. H. Chong *et al.*, "Frequent premature atrial complexes predict new occurrence of atrial fibrillation and adverse cardiovascular events," *Europace*, vol. 14, no. 7, pp. 942–947, 2012.

[2] B. T. Huang *et al.*, "Relation of premature atrial complexes with stroke and death: Systematic review and meta-analysis," *Clin. Cardiol.*, vol. 40, no. 11, pp. 962–969, 2017.

[3] B. S. Larsen, P. Kumarathurai, J. Falkenberg, O. W. Nielsen, and A. Sajadieh, "Excessive Atrial Ectopy and Short Atrial Runs Increase the Risk of Stroke beyond Incident Atrial Fibrillation," *J. Am. Coll. Cardiol.*, vol. 66, no. 3, pp. 232–241, 2015.

Automated Framework for the Augmentation of Missing Anatomical Structures and Generation of Personalized Atrial Models from Clinical Data

Luca Azzolin

Introduction

Personalized computational models are often generated from electroanatomical maps, which might lack important anatomical structures like the appendages, or from imaging data which are potentially affected by segmentation uncertainty. A bi-atrial statistical shape model (SSM) was shown to cover atrial shape variability. We hypothesized that it could, therefore, also be used to infer the shape of missing structures and deliver ready-to-use models to assess atrial fibrillation vulnerability in silico.

Material and Methods

We implemented a highly automatized pipeline to generate a personalized computational model by fitting the SSM to the clinically acquired geometries. We applied our framework to a geometry coming from an electroanatomical map and one derived from magnetic resonance images (MRI). Only landmarks belonging to the left atrium and no information from the right atrium were used in the fitting process.

Results

The left atrium surface-to-surface distance between electroanatomical map and a fitted instance of the SSM was 2.26±1.95 mm. The distance between MRI segmentation and SSM was 2.07±1.56 mm and 3.59±2.84 mm in the left and right atrium, respectively.

Discussion and Conclusions

Our semi-automatic pipeline provides personalized computational models representing the original anatomy well by fitting a SSM. We were able to infer the shape of the right atrium even in the case of using information only from the left atrium.

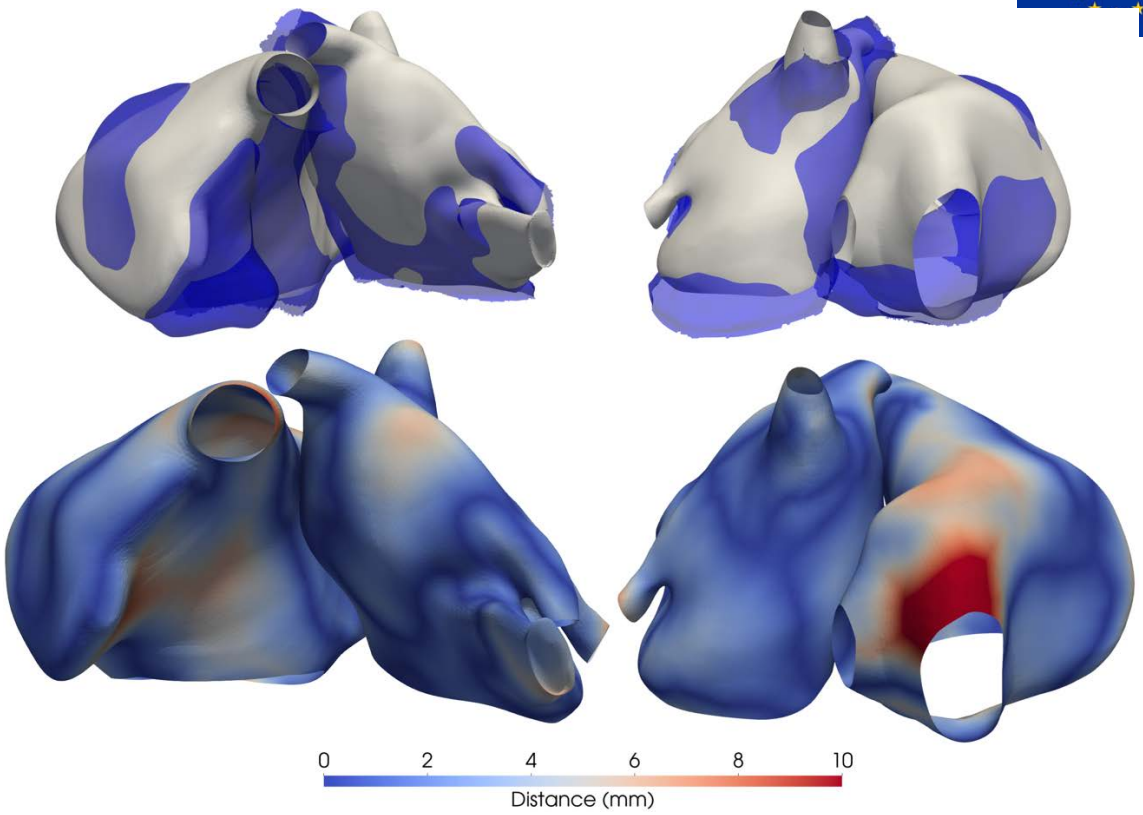

Figure: Top row: anterior (left) and posterior view (right) of the best fitting SSM instance (grey) to the target MRI segmentation (semi-tansparent blue). Bottom row: anterior and posterior view of the surface-to-surface distance between fitted SSM instance and target mesh shown on the fitted SSM instance.

Rotor Termination in Cholinergic Paroxysmal Atrial Fibrillation by SK Channels Inhibition and Isoproterenol: a Computational Study

Chiara Celotto

Introduction

Hyperactivity of the parasympathetic nervous system has been linked to the onset of paroxysmal atrial fibrillation (AF) [1]. Recent investigations have proven inhibition of small-conductance calcium-activated potassium (SK) channels to improve adverse cholinergic effects in the atria [2]. It has also been reported that β-adrenergic stimulation by Isoproterenol (Iso) can act as a brake to lessen cholinergic effects on atrial tissue [3]. Furthermore, the combination of SK channel block (SKb) and Iso has been suggested to possibly prolong atrial APD in ACh-stimulated myocytes [4].

Material and Methods

In this study, computational modeling was used to test individual and combined effects of SKb and Iso in terminating a stable rotor in a cholinergic AF model of human atria. 2D tissues with uniform ACh concentrations of 0.01 or 0.1 µM were simulated. After stable rotors were initiated, 1 µM Iso and/or complete SKb were progressively applied over time following different application kinetics.

Results

Both Iso alone and the combination of Iso and SKb were able to terminate rotors for the two ACh concentrations. SKb was only able to terminate the rotor for the lower ACh concentration.

Discussion and Conclusions

In conclusion, the results from this study support β-adrenergic stimulation and SK channel block, the latter with less efficacy, as potential options to terminate rotors in parasympathetically-stimulated human atria.

References

[1] Iso K, Okumura Y, Watanabe I, Nagashima K, Takahashi K, Arai M, Watanabe R, Wakamatsu Y, Otsuka N, Yagyu S, Kurokawa S, Nakai T, Ohkubo K, Hirayama A. Is Vagal Response During Left Atrial Ganglionated Plexi Stimulation a Normal Phenomenon? Circulation Arrhythmia and Electrophysiology October 2019;12(10):e007281.

[2] Chen PS, Chen LS, Fishbein MC, Lin SF, Nattel S. Role of the Autonomic Nervous System in Atrial Fibrillation. Circulation Research April 2014;114(9):1500–1515.

[3] Sosunov EA, Anyukhovsky EP, Rosen MR. Adrenergic-Cholinergic Interaction that Modulates Repolarization in the Atrium is Altered with Aging. Journal of Cardiovascular Electrophysiology April 2002;13(4):374–379. ISSN1045-3873.

[4] Celotto C, Sanchez C, Mountris KA, Laguna P, Pueyo E. SK Channel Block and Adrenergic Stimulation Counter-act Acetylcholine-Induced Arrhythmogenic Effects in Human Atria. In 2020 42nd Annual International Conference of the IEEE Engineering in Medicine & Biology Society (EMBC). Montreal, QC, Canada: IEEE. ISBN9781728119908, July 2020;2303–2306.

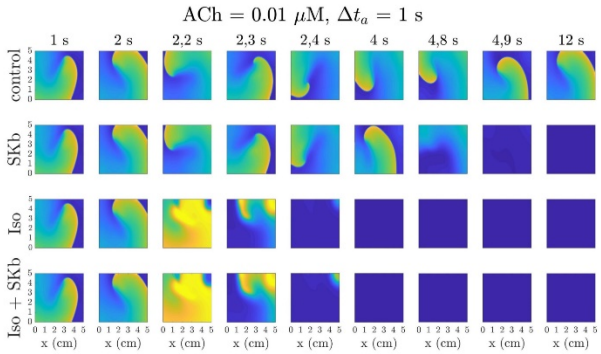

Figure 1: Time for rotor termination in the different simulated cases. The vertical black line represents the start time of Iso and SKb application.

Analysis of Unipolar Electrogram Eigenvalue Dispersion for the Detection of Atrial Fibrosis

Jennifer Riccio

Background

Atrial fibrosis plays a meaningful role in the pathogenesis of atrial fibrillation (AF). Areas with peak-to-peak amplitude of bipolar electrograms (b-EGMs) lower than 0.5 mV are detected as scar tissue and targeted for AF ablation procedures. However, this approach disregards the spatiotemporal information held in the signal and is influenced by b-EGMs dependence on catheter orientation.

Objective

To overcome these limitations, in this study, we propose to use the dominant-to-remaining eigenvalue dominance ratio (EIGDR) of unipolar electrograms (u-EGMs) within a group of nearby electrodes (clique) as a measure of the voltage wavefront roughness and correlate it with the presence of fibrosis.

Methods

We simulated u-EGMs from a 2D atrial tissue, including a circular patch of diffuse fibrosis, following the Courtemanche model. They were corrupted with one hundred different realizations of real noise with level $\sigma_n = 33\ \mu V$. One hundred different maps of three EIGDRs (R: ratio of first eigenvalue of u-EGMs correlation matrix to the sum of all the others; R^A: same ratio after u-EGMs time alignment within the clique; and ΔR^A: the gain in eigenvalue concentration produced by alignment) were obtained using two clique sizes (3×3 and 2×2) and three catheter orientations ($0°, 30°\ and\ 45°$). The maximum accuracy for fibrosis detection (ACC) was used as performance measurement. The threshold for maximum accuracy was obtained jointly for the three orientations, assuming that the angle between the propagation direction and the catheter is not known a priori. For performance comparison, maps of peak-to-peak voltage of b-EGMs in each of the two catheter directions (V^{b-x} and V^{b-y}) and of their maximum (V^{b-m}) were also tested.

Results

The proposed EIGDR indices show the following average performance (mean $\pm$ standard deviation): ACC = 0.84 $\pm$0.01, 0.88 $\pm$ 0.01 and 0.80 $\pm$\$ 0.02 for R, R^A and ΔR^A, respectively, when 2×2 cliques are used. With the 3×3 configuration, ACC = 0.87 $\pm$ 0.02, 0.95 $\pm$ 0.02 and 0.88 $\pm$ 0.02 for the same indices. Bipolar voltage maps achieve ACC = 0.69 $\pm$0, 0.86 $\pm$0.01 and 0.91 $\pm$0.01, for V^{b-x}, V^{b-y} and V^{b-m}, respectively.

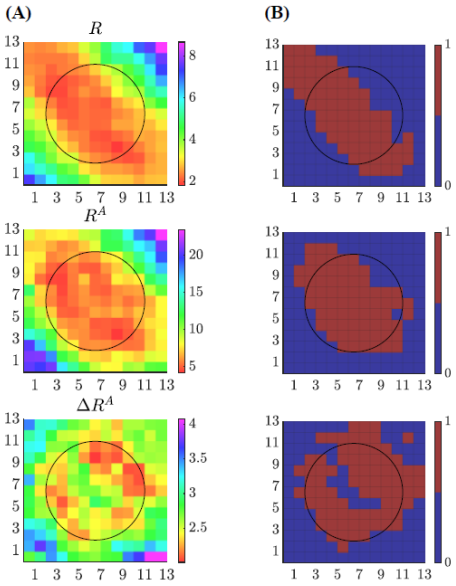

Figure 7: (A): EIGDR maps for 3×3 cliques and 45° catheter for one noise realization. (B): identification masks for ACC thresholds.

Discussion

EIGDR approach allows to discriminate fibrotic from non-fibrotic tissue, improving its performance when clique alignment is considered and 3×3 configuration is used, providing slightly improved performance to standard voltage maps for the 3×3 aligned EIGDR maps.